Competition between Cholesterol and Phosphatidylcholine for the Hydrophobic Surface of Sarcoplasmic Reticulum Ca^{2+}-ATPase†

John R. Silvius,‡ Debra A. McMillen, Neil D. Saley, Patricia C. Jost,* and O. Hayes Griffith*

ABSTRACT: A multiple equilibrium binding model is used to examine phospholipid and cholesterol binding with the transmembranous protein Ca^{2+}-ATPase (calcium pump). The protein was reconstituted in egg phosphatidylcholine bilayers by lipid substitution of rabbit muscle sarcoplasmic reticulum. Electron spin resonance spectra of a phosphatidylcholine spin-label and a recently developed cholesterol spin-label show two major spectral contributions, a motionally restricted component consistent with interactions between the label and the protein surface and another component characteristic of motion of the label in a fluid lipid bilayer. The number of lipid binding (or contact) sites at the hydrophobic surface of the protein is calculated to be $N = 22 \pm 2$. Experiments with intact sarcoplasmic reticulum membranes give approximately the same value for N. The relative binding constants are $K_{av} \sim 1$ for the phosphatidylcholine label and $K_{av} \sim 0.65$ for the cholesterol spin-label. Thus, cholesterol does contact the surface of the protein, but with a somewhat lower probability than phosphatidylcholine. This is confirmed by competition experiments where unlabeled cholesterol and the phospholipid spin-label are both present in the bilayer. Evidently the flexible acyl chains of the phospholipid molecules accommodate more readily to the irregular surface of the protein than does the rigid steroid structure of cholesterol.

In recent years, several integral membrane proteins have been studied by a variety of physical techniques to provide information about the dynamics and functional consequences of lipid–protein interactions. One of the most extensively studied proteins is the Ca^{2+}-activated adenosinetriphosphatase (Ca-ATPase[1] or calcium pump protein) of mammalian sarcoplasmic reticulum.

The influence of the Ca-ATPase on properties of the membrane lipids has been studied by electron spin resonance (ESR) of spin-labeled lipids (Hesketh et al., 1976; Jost & Griffith, 1978a; Thomas et al., 1982; McIntyre et al., 1982), by ^1H, ^2H, and ^{31}P nuclear magnetic resonance (NMR) (Rice et al., 1979; Seelig et al., 1981; Deese et al., 1982; McLaughlin et al., 1981), fluorescence (Moore et al., 1978; London & Feigenson, 1981), and differential scanning calorimetry (Gomez-Fernandez et al., 1980). The findings of studies with techniques having short time scales (10^{-7}–10^{-9} s) such as ESR and fluorescence are compatible with the idea that lipids experience two distinguishable environments when protein is present. Techniques with longer time scales (10^{-3}–10^{-5} s) such as NMR observe a single average environment. In addition the spin-labeling experiments indicate that the labeled lipid in contact with the protein is motion restricted and that the influence of the protein on the bilayer falls off rapidly in successive lipid layers away from the protein (Jost & Griffith, 1978a).

These results are supplemented by the findings of studies investigating the importance of lipids for the function of the Ca-ATPase in the membrane environment. While a variety of phospholipid species and even some nonphospholipid amphiphilic molecules can support Ca-ATPase activity to some extent (Dean & Tanford, 1977; Bennett et al., 1978), the activity varies depending on the composition of the lipid environment. On the other hand, lipid or detergent species with rigid hydrocarbon skeletons such as cholesterol or cholate do not support activity (Hardwick & Green, 1974; Warren et al., 1974a; Hesketh et al., 1976).

The analysis of both dynamic and functional studies of the Ca-ATPase in lipid membranes can benefit from knowledge of basic thermodynamic parameters describing the Ca-ATPase–lipid interactions. Among the most important of these parameters are the number of lipids directly associated with the Ca-ATPase (N) and the relative binding affinity (K) of the enzyme for lipids of very different structures. These quantities can be estimated by using a multiple binding equilibrium analysis (Griffith & Jost, 1979) that considers the exchange of one type of lipid (L*) for another (L) at each of N sites on the hydrophobic surface of the protein (P):

$$L^* + PL_{N-i}L^*_i \rightleftharpoons L + PL_{N-i-1}L^*_{i+1} \qquad (1)$$

Any binding site is always occupied by either L or L* since the equilibrium exchange occurs at the hydrophobic interface between the protein and lipid bilayer.

The application of this type of multiple equilibria binding formalism in membrane biochemistry is relatively new and differs from the classical treatment of water-soluble enzymes because the solvent that is treated explicitly in the equations is the lipid bilayer and not water. The work thus far has concentrated on phospholipid equilibrium binding, and the picture emerging from preliminary work on several integral membrane enzymes, including the Ca-ATPase, is that most phospholipids occupy simple nondiscriminating contact sites serving to solvate the protein hydrophobic surface; i.e., the relative binding constant is approximately unity ($K \sim 1$). Although most of the phospholipids appear to be rapidly interchangeable at the protein surface, some phospholipid species

† From the Institute of Molecular Biology, University of Oregon, Eugene, Oregon 97403. *Received March 15, 1983; revised manuscript received August 18, 1983.* This work was supported by U.S. Public Health Service Grant GM 25698 and a fellowship from the Medical Research Council of Canada to J.R.S.

‡ Present address: Department of Biochemistry, McGill University, Montreal PQ, Canada H36 1Y6.

[1] Abbreviations: Ca-ATPase, Ca^{2+}-activated adenosinetriphosphatase (the calcium pump protein); Ch, cholesterol; Ch*, 17-spiroxylcholesterol nitroxide; ESR, electron spin resonance; NMR, nuclear magnetic resonance; PC, phosphatidylcholine; PC*, 1-palmitoyl-2-(14-proxylstearoyl)-*sn*-3-phosphatidylcholine (14-proxylphosphatidylcholine); SR, sarcoplasmic reticulum; MOPS, 4-morpholinepropanesulfonic acid; EDTA, ethylenediaminetetraacetic acid; DTT, dithiothreitol; Tris, tris(hydroxymethyl)aminomethane; SDS, sodium dodecyl sulfate.

0006-2960/84/0423-0538$01.50/0

involved in function can have large relative binding constants (Brotherus et al., 1981; London & Feigenson, 1981; Knowles et al., 1981; Cable & Powell, 1980; Griffith et al., 1982a; Marsh & Watts, 1982).

An early study (Warren et al., 1975), based on activity measurements, suggested that cholesterol is excluded from the boundary layer directly contacting the Ca-ATPase; that is, $K = 0$ for cholesterol association with the ATPase when enough phospholipid is present to solvate the enzyme. While cholesterol is at best a minor component of the sarcoplasmic reticulum membrane (Sanslone et al., 1972), this early study addressed an important question regarding the properties of the lipid–protein interface. The Ca-ATPase is widely considered to be a typical integral membrane protein, and cholesterol is a biologically important lipid in eukaryotic membranes. The behavior of cholesterol with respect to the hydrophobic protein surface provides useful information about the lipid–protein interface.

The equilibrium behavior of cholesterol gives information about the molecular fit at the lipid–protein interface, hence the geometry of the hydrophobic protein surface. Also, some fairly rigid rodlike molecules (such as diphenylhexatriene) are widely used to characterize membranes, and it is important to know, a priori, if rigid molecules are excluded from contact with the protein surface.

There has been no direct characterization of cholesterol–protein interactions using equilibrium binding measurements. The purpose of this study is to address the question of whether cholesterol is interchangeable with phospholipid for solvating the hydrophobic surface of the Ca-ATPase. A preliminary report of some of this work has been included in a recent review (Griffith et al., 1982a).

Materials and Methods

Materials. Phosphatidylcholine (PC) was isolated from hen egg yolk as described by Singleton et al. (1965), incorporating 5 mg/L butylated hydroxytoluene (BHT) in all solvents used for lipid extraction and chromatography to minimize lipid oxidation. Chromatographically purified egg PC was twice precipitated from hexane by slowly adding 10 volumes of cold acetone to remove residual BHT from the lipid, which was then stored at −20 °C under argon. Cholic acid (Aldrich Chemical Co.) was twice treated with decolorizing charcoal and then recrystallized 3–4 times from ethanol (10 g of cholic acid/100 mL of 95% ethanol) to give a colorless and chromatographically homogeneous product, which was then neutralized with equimolar KOH. Octyl glucoside was synthesized by the method of Roman & Keana (1978) and repurified shortly before use by silicic acid column chromatography and recrystallization from acetone.

The 2-(14-proxylstearoyl)phosphatidylcholine spin-label (Figure 1, I) and a novel cholesterol spin-label (Figure 1, II) were synthesized by using previously described procedures (Keana, 1979; Keana et al., 1981, 1982). Cholesterol (Sigma grade) was obtained from Sigma Chemical Co. and used without further purification. Chloroform was routinely redistilled prior to use; all other chemicals used were of reagent grade or better.

Lipid Substitution and Reconstitution of Ca-ATPase. Sarcoplasmic reticulum (SR) vesicles were prepared from the white muscles of rabbit hindlimbs essentially as described by Eletr & Inesi (1972), replacing histidine with MOPS as buffer and omitting EDTA from the homogenizing medium; low-speed centrifugations were run at 8000*g* for 20 min. The specific activities, lipid/protein ratios, and polypeptide compositions of these SR preparations were comparable to those

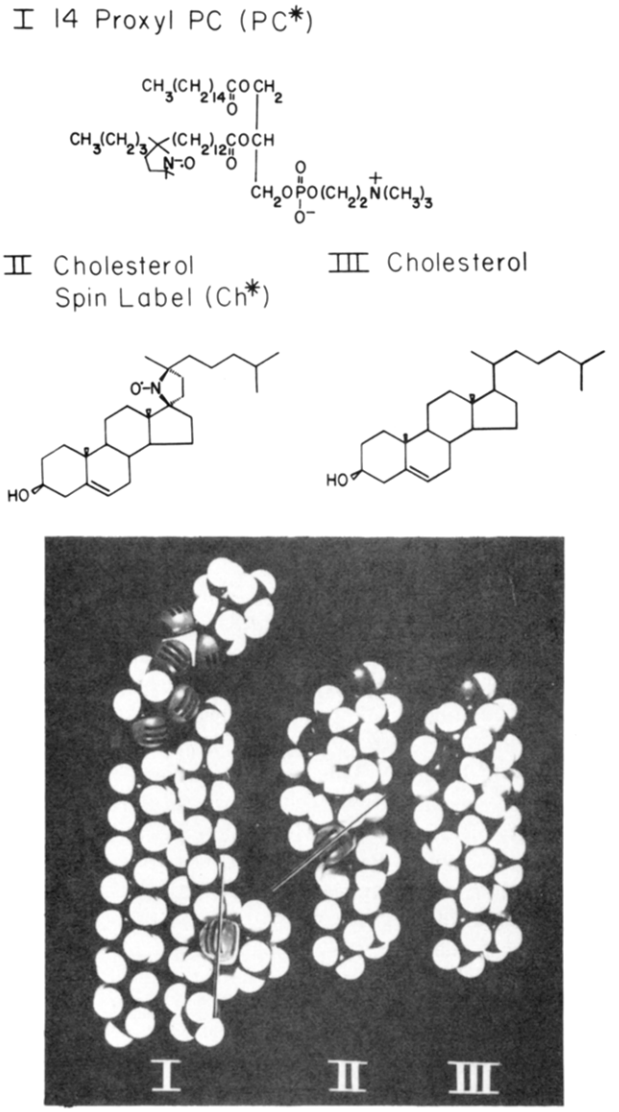

FIGURE 1: Structures of the phospholipid (I, PC*) and cholesterol spin-label (II, Ch*) used in this study. The structure of cholesterol (III) is shown for comparison with the cholesterol spin-label. The space-filling molecules are shown below. The bars on I and II indicate the direction of the nitroxide *z* axis.

reported by other workers (Eletr & Inesi, 1972; MacLennan, 1974; Meissner, 1974; Warren et al., 1974a).

The reconstitution of the Ca-ATPase in defined lipids involved two steps. In the first step, the Ca-ATPase was simultaneously lipid exchanged and purified by a modification of the centrifugation procedure of Warren et al. (1974a,b). In a typical preparation sarcoplasmic reticulum membranes (7 mg of protein) were incubated for 30 min at 0 °C with 30 μmol of PC and 65 μmol of cholate in 1.0 mL of incubation buffer (1 M KCl, 50 mM K_2HPO_4, and 1 mM each of $MgCl_2$, ATP, and DTT, pH 8.0) containing 0.25 M sucrose. The mixture was centrifuged at 160000*g* for 14–18 h at 4 °C into a linear gradient of 20–60% sucrose in the incubation buffer. The sharp turbid band, normally found at 35–40% sucrose and containing 45–60% of the applied protein, was recovered. (The recovered material contained 0.30–0.35 μmol of lipid phosphorus/mg of protein and had a Ca-ATPase specific activity of ~10 μmol of P_i mg^{-1} min^{-1} at 35 °C.) Champeil et al. (1981) have shown that the ATPase can be inactivated by the high pressures experienced during ultracentrifugation unless protected against inactivation by the presence of sucrose (0.3 M) or ATP. Our procedures did include sucrose (>0.3 M) or the combination of ATP and (≥0.25 M) sucrose.

In the second step of the reconstitution procedure, a mixture of spin-label (~0.4 label/ATPase), any extra lipid desired, and octyl glucoside at a level just sufficient to sharply reduce the turbidity of the preparation was added at 0 °C. The needed amount of octyl glucoside can be approximately calculated as 4.5 mg/mL plus 1.2 mg/μmol of added lipid. Care was taken to avoid the use of excessive amounts of octyl glucoside, as higher levels of the detergent can diminish the final ATPase activity recovered (Banerjee et al., 1979). After 15 s the sample was diluted over ~30-s interval with an equal volume of 0.25 M sucrose incubation buffer, increasing the turbidity sharply. The diluted sample was chromatographed on Sephadex G-150 in the same buffer to remove cholate and octyl glucoside (Stoffel et al., 1977; Mimms et al., 1981). The turbid void volume fractions were centrifuged for 8–12 h at 160000*g*, 4 °C, onto a pad of 55% sucrose, 100 mM KCl, 5 mM MOPS, and 1 mM DTT, pH 7.5. The band over the sucrose was recovered and pelleted through a layer of 22% sucrose in the same KCl/MOPS/DTT buffer (2 h, 100000*g*, 4 °C).

Analytical Methods. Protein was assayed essentially by the method of Lowry et al. (1951), after solubilization of the Ca-ATPase samples with 2.5% sodium dodecyl sulfate. Bovine serum albumin (Miles Pentex; fraction V, fatty acid poor) was used as the standard. Phospholipid was extracted by the method of Bligh & Dyer (1959) and phosphorus assayed by the method of Lowry & Tinsley (1974). Phospholipid composition was determined by two-dimensional thin-layer chromatography on silica gel G (Merck) analytical plates using the solvent system of Parsons & Patton (1967). Ca^{2+}-dependent ATPase activity was measured by using the assay conditions described by MacLennan (1974), with MOPS replacing Tris as the buffer. Released inorganic phosphate was determined as described previously (Brotherus et al., 1979). Samples for electron microscopy were negatively stained with 2% potassium phosphotungstate at pH 7.2. Sodium dodecyl sulfate–polyacrylamide disc gel electrophoresis was performed by the method of Laemmli (1970) as described by Meissner (1974). The separating gel contained 7.5% acrylamide and 0.2% bis(acrylamide), with the stacking gel containing 3% acrylamide and 0.08% bis(acrylamide). Samples (typically 100 μg of protein) were dissociated in 4 M urea, 2% sodium dodecyl sulfate, 60 mM Tris, and 3% β-mercaptoethanol, pH 6.8, with heating to 100 °C for 4 min. Gels were stained for protein with Coomassie Blue.

ESR Measurements. ESR spectra were collected on a Varian E-line 9.5 GHz spectrometer interfaced with a 32K Varian 620/L100 computer. The sample temperature of 25 °C was monitored by a thermocouple inserted into the cavity at the level of the sample before and after the ESR run; temperature was controlled to ~ ±0.1 °C. Spectra were typically collected at a power setting of 5 mW with scan times of 20–30 min, filter time constant of 0.1 s, modulation amplitudes of 0.8–1.25 G (depending on line width), and a scan range of 100 G. Base-line adjustments, integrations, and subtractions of the digitized spectra were carried out as previously described (Jost & Griffith, 1978b; Brotherus et al., 1980).

Results

Characterization of the Reconstituted Ca-ATPase. The Ca-ATPase preparations, obtained from the cholate-mediated lipid exchange followed by sucrose gradient centrifugation, contained a relatively constant lipid/protein ratio of 0.33–0.37 μmol of lipid phosphorus/mg of protein which is equivalent to 38–43 phospholipids per Ca-ATPase of M_r 115000.

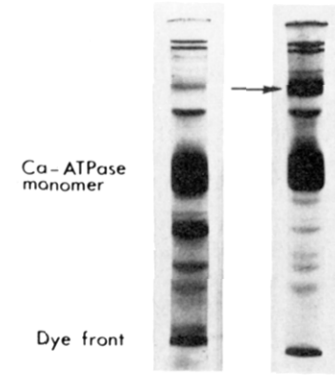

FIGURE 2: SDS–polyacrylamide gel electrophoresis of the sarcoplasmic reticulum (left) and a reconstituted sample (right). The dominant protein present in both gels is the Ca-ATPase monomer, and the reconstituted sample shows substantially more homogeneity in protein composition. The band indicated by the arrow appears to represent an oligomeric form of the Ca-ATPase, which is an artifact that arises when samples are dissociated at 100 °C prior to electrophoresis (Banerjee et al., 1979).

Two-dimensional thin-layer chromatography followed by phosphate analysis showed that >97% of the lipid was PC. Egg PC was chosen as the phospholipid for our reconstitutions because it is easily purified in the relatively large quantities needed and because it is a single phospholipid head-group species with predominately α-saturated, β-unsaturated acyl chains. The average acyl chain lengths and degree of unsaturation approximate those of PC from SR (cf. Marai et al., 1973; Bangham et al., 1974).

The final yield of protein from preparations after the second reconstitution step (when lipid was added in octyl glucoside, followed by dilution and gel filtration) was ~50% based on the amount of SR protein used as the starting material for the two-stage reconstitution. As shown in Figure 2, the final reconstitutions have a more homogeneous protein composition (>90% Ca-ATPase) than does the native SR, based on Coomassie Blue staining intensity. The lipid content of the reconstituted samples was proportional to the amount of lipid added in the second reconstitution stage, as shown in Figure 3. This overall procedure allows good control of the lipid/protein ratio of the final preparation over a range of values that includes our native SR value of 0.7 μmol of phospholipid/mg of ATPase. The final preparations gave a single sharp band on linear sucrose gradients. Electron microscopy of a negatively stained reconstituted sample with a near-physiological lipid/protein ratio showed unilamellar vesicles with diameters ranging from 600 to 2500 Å, a size range also seen in the micrographs of the control samples of native SR vesicles. The specific activities of the reconstituted Ca-ATPase vesicles ranged from 4 to 10 μmol of ATP hydrolyzed min^{-1} (mg of protein)$^{-1}$ as their lipid contents rose from 0.35 to 1.7 μmol of phospholipid/ATPase (roughly, from half to twice the physiological lipid level). Moore et al. (1978) and Wang et al. (1979) have observed a similar variation of ATPase activity with lipid/protein ratio in reconstituted or partially delipidated samples of sarcoplasmic reticulum. In the present study, native SR (with ~79 mol of PL/mol of ATPase), when assayed under the same conditions, had an ATPase specific activity of 4–4.5 μmol of ATP hydrolyzed min^{-1} (mg of protein)$^{-1}$.

ESR Spectra and Data Analysis of 14-Proxyl-phosphatidylcholine Spin-Label. Figure 4 shows representative experimental line shapes from a series of egg PC reconstituted samples of Ca-ATPase as a function of the lipid/protein ratio. The composite nature of this spectral series is most clearly evident in the top two spectra, which were

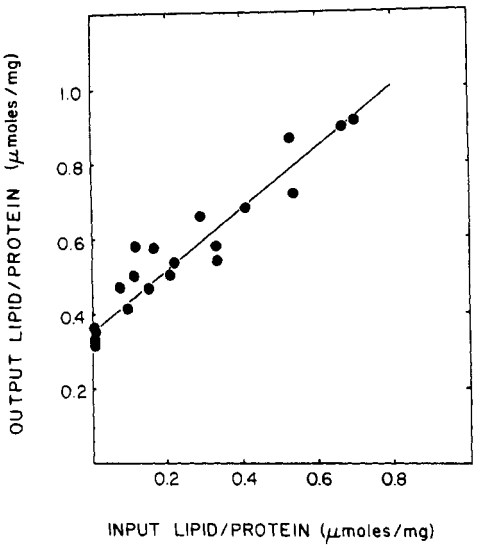

FIGURE 3: Final lipid/protein ratios of the reconstituted Ca-ATPase achieved by varying the amount of extra lipid added to the cholate-mediated lipid-exchanged Ca-ATPase as a function of added lipid. Lipid-exchanged Ca-ATPase (containing 0.30–0.35 μmol of egg PC/mg of protein) was combined with a defined amount of lipid (input) in octyl glucoside at a detergent level determined by the sample volume and the amount of added lipid (see Materials and Methods). The lipid/protein ratios of the final reconstituted preparations, obtained by subsequent gel filtration and centrifugation as described in the text, are plotted on the *y* axis (output) vs. the extra added lipid (input). The least-squares line shown has a slope of 0.8, while complete recovery of the added lipid in the reconstituted preparations would give a slope of 1.0. A portion of the vertical point scatter can be attributed to variation in the lipid/protein ratio of the lipid-exchanged Ca-ATPase preparations used as the starting material for this second reconstitution step.

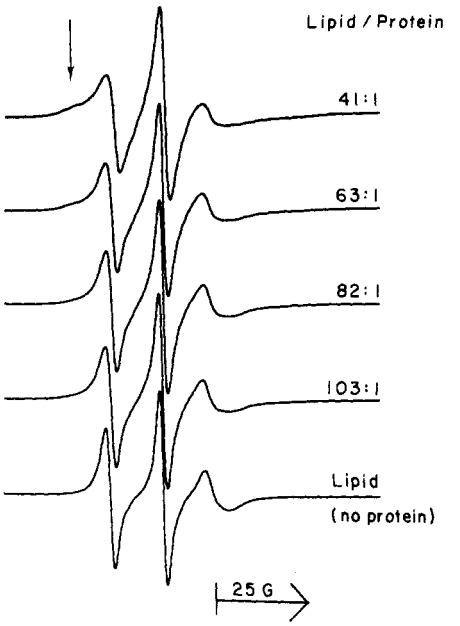

FIGURE 4: Representative ESR spectra of the phosphatidylcholine spin-label (PC*) in samples of Ca-ATPase which have been lipid exchanged and reconstituted with egg PC. The molar ratio of lipid to protein for each sample is indicated on the right. The labeling level was ~0.4 PC* per ATPase for all samples. These spectra were recorded at 25 °C and have been normalized to the same arbitrary center peak intensity. The bottom spectrum is that of PC* in egg PC at a molar labeling ratio of 1/150.

obtained from samples containing high protein content. An underlying broad spectral component (see arrow) comprises 50%, 35%, 25%, 22%, and 0% of the spectra, respectively, from top to bottom. These percentages were arrived at by the

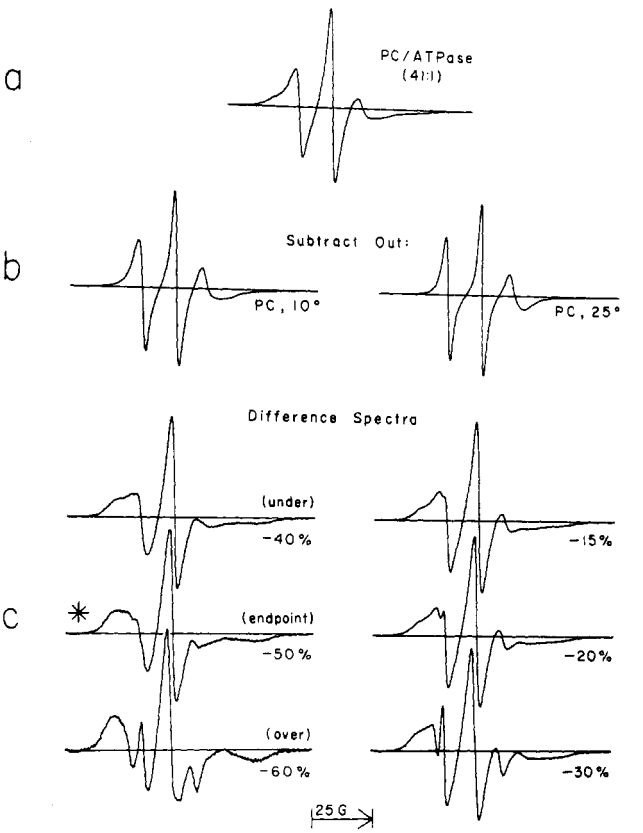

FIGURE 5: Procedure for obtaining the line shape of the broad spectral component (bound line shape): (a) the experimental ESR spectrum of PC* in a PC reconstitution of Ca-ATPase at lipid to protein molar ratio of 41/1 recorded at 25 °C; (b) experimental ESR spectra of PC* in egg PC liposomes recorded at two temperatures, 10 (left) and 25 °C (right); (c) two sets of difference spectra obtained by incremental subtractions of the PC model system at 10 (left) and 25 °C (right). The correct end point line shape is starred and shows that approximately 50% of the absorption of spectrum a is due to the broad component. This reference line shape was then used to analyze all of the PC*–PC–ATPase recombinants at 25 °C. All spectra are plotted to a constant center line height, and the percentages removed to obtain the difference spectra are normalized to the integrated intensities.

procedures illustrated in Figures 5 and 6. A key step is determining the line shape of the underlying broad spectral component (Figure 6b). This bound line shape is obtained by the steps outlined in Figure 5. The general approach is to use the spectrum of a model lipid system to approximate the bilayer component and then to subtract this spectrum from an experimental spectrum of a sample with relatively high protein content to yield difference spectra. The presence of protein, in our experience, always somewhat broadens the bilayer line, with the extent of the broadening being a function of the protein content (Jost & Griffith, 1978a; Marsh et al., 1978). Therefore, the bilayer component is simulated by the egg PC model lipid system at a somewhat lower temperature. The matching bilayer line width is chosen by trial and error on the basis of incremental spectral subtractions. Two criteria are used: (1) the bilayer component is completely removed at the end point, and (2) the remaining homogeneous broad line shape can be matched by an experimental or theoretical spectrum. The left column of Figure 5 illustrates the correct choice of the bilayer component b (PC* in egg PC vesicles at 10 °C) which, when incrementally subtracted from the experimental spectrum a, yields a series of difference spectra, some of which are shown in spectrum c. The end point spectrum is starred, and the under- or oversubtractions yield obvious line-shape distortions. On the right are shown the

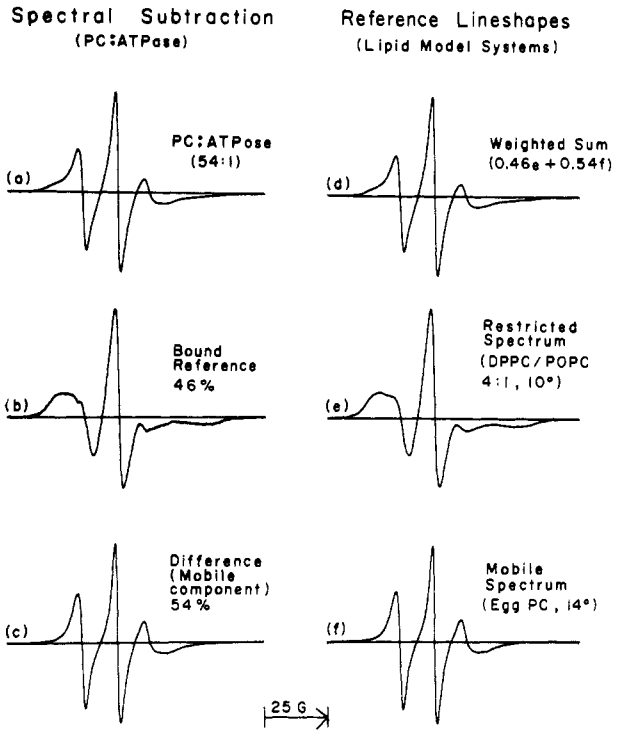

FIGURE 6: Illustration of the PC* spectral data analysis used to obtain values needed for the equilibrium binding treatment. The experimental composite spectrum a minus the bound reference spectrum b yields the difference spectrum c. As a check on these line shapes, matching reference spectra are shown on the right. Spectrum d is a weighted sum of the lipid model system spectra e and f, where the weighting factors were obtained from the subtraction sequence on the left. Spectrum f was also used as the criterion for the subtraction end point. There is a very good match between the pairs of spectra in the left and right columns.

results of choosing a bilayer line shape that is too narrow (egg PC–PC* recorded at 25 °C, the same temperature as the membrane sample). In this case, as expected, none of the difference spectra meet either of the criteria for a reasonable end point.

The left column of Figure 6 is a representative analysis of one of the experimental spectra a, where the bound line-shape b has been subtracted to yield the bilayer difference spectrum c. The final end point spectrum must be real and undistorted, i.e., match the line shape of an experimental bilayer spectrum, which for this case is shown in Figure 6f. (The sole end point criterion of avoiding a negative base-line deflection may lead to oversubtractions depending on the temperature, position of the spin-label, amount of protein, and the splitting of the bound component). Quantitatively, this procedure shows that the original experimental spectrum a is composed of about 46% of the motion-restricted component b and 54% of the mobile component c. The experimental spectrum a can be regenerated (d) by summing the experimental reference spectra (e and f). Reference line-shape e is from a lipid mixture that is in the gel phase with little or no liquid-crystalline lipid present, as determined from the phase diagram of Davis et al. (1980), and was available in our files of reference spectra. All three line shapes of the right column are a very good fit to the corresponding line shapes of the left column of Figure 6.

Multiple Equilibrium Binding Model Yields the Number of Sites (N) and the Average Relative Binding Affinity (K_{av}). The spectroscopic data and analysis described above, combined with the multiple equilibrium binding treatment of Brotherus et al. (1981), give the more familiar and generally useful quantities N and K_{av}. Since each binding or contact site is

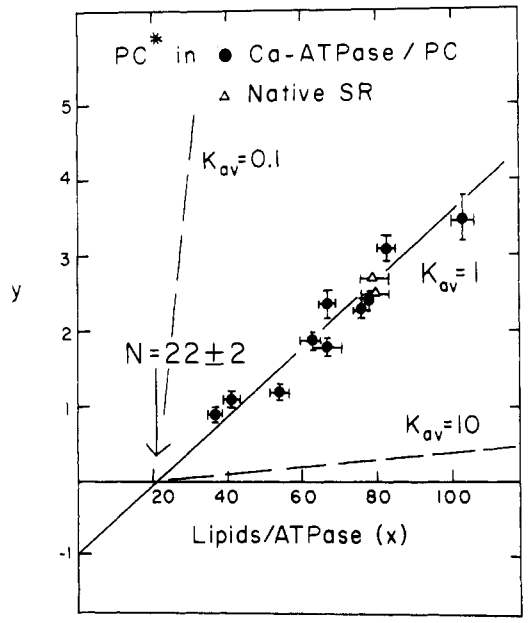

FIGURE 7: Experimental binding curve for the interaction of PC* with the Ca-ATPase reconstituted in an egg PC background (solid circles) and in native SR (open triangles). The ratio of free to bound spin-label (y) is plotted vs. the molar ratio of lipid to Ca-ATPase (x). The line fit to the experimental data corresponds to the number of binding sites N = 22 (assuming a molecular weight of 115 000 for the Ca-ATPase) and a relative binding constant K_{av} = 1. For comparison, K_{av} = 0.1 and K_{av} = 10 are indicated.

assumed to be independent of all others, eq 1 can be written in terms of binding sites, B

$$L^* + BL \rightleftharpoons L + BL^* \tag{2}$$

$$K = \frac{L_f L_b^*}{L_b L_f^*} \tag{3}$$

where L_f and L_b are moles of free and bound solvent lipids and L_f^* and L_b^* are moles of free and bound solute lipid (i.e., the spin-labeled lipid). Where more than one class of binding sites is involved, it is useful to define the weighted average binding constant over the m classes of sites as

$$K_{av} = \frac{1}{N}\sum_{i=1}^{m} n_i K_i \tag{4}$$

When $L^* \ll L$, it can be shown that

$$y = \frac{x}{NK_{av}} - \frac{1}{K_{av}} \tag{5}$$

where $y = L_f^*/L_b^*$ and x = molar ratio of lipid/protein. The plot of y (ESR data) vs. x (compositional data) for PC*-labeled samples is shown in Figure 7. Within experimental error the multiple equilibrium binding treatment shows a linear relationship between y and x as predicted. The x intercept of the plot in Figure 7 gives the total number of lipids in momentary contact with the protein. The y intercept corresponds to $-1/K_{av}$, and the slope is $1/(NK_{av})$. The value of N obtained from these PC* data is 22 ± 2, and $K_{av} \sim 1$. K_{av} is measured relative to the solvent lipid (just as the binding of a water-soluble ligand is referenced to the binding of water). The solvent lipid in this case is egg PC, and the solute is the spin-label PC*; thus, $K_{av} \sim 1$ indicates PC* and PC behave the same with respect to equilibrium association with the protein.

Cholesterol at the Lipid–Protein Interface. To examine the interaction of cholesterol with the Ca-ATPase, the association

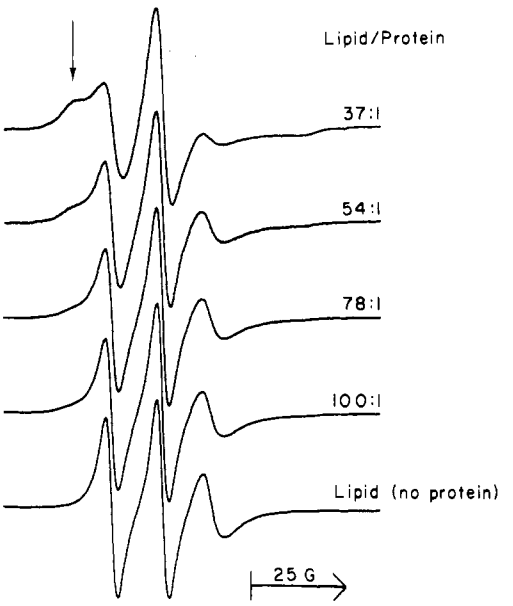

FIGURE 8: Representative ESR spectra of the cholesterol spin-label (Ch*) in samples of Ca-ATPase of increasing lipid (egg PC) content. These samples are parallel to those of Figure 4 except for the spin-label used. The labeling level is ~0.4 Ch* per ATPase, and spectra were recorded at 25 °C and plotted to arbitrary center line height. The bottom spectrum is that of Ch* in egg PC at a molar labeling ratio of 1/150.

of the spin-labeled cholesterol analogue Ch* (Figure 1, label II) with the protein was measured. The long molecular axis of this molecule lies approximately in the y,z plane and is at an angle of approximately 40° to the nitroxide y axis. (In the standard convention the axis exhibiting the largest splitting, the z axis, is parallel to the nitrogen $2p_z$ orbital associated with the unpaired electron, the x axis lies along the N–O bond, and y is perpendicular to x and z). In lipid bilayers, the motional behavior of this molecule is sufficiently close to the case of y-axis rotation that the line shapes observed depend largely on the degree of restriction of its axial rotation (Van et al., 1974). A series of spectra of the cholesterol label (II) in egg PC bilayers at temperatures ranging from −10 to 30 °C was collected to furnish representative model system line shapes corresponding to varying degrees of restriction of axial rotation. The spectra shown in Figure 8 (bottom) and Figure 9e,f are from this series. The spectra of Figure 9e,f illustrate cases of substantially restricted rotation about the long steroid axis (reduced averaging of the nitroxide z-axial tensor element) and rapid rotation (nearly complete averaging), respectively.

The series of spectra shown in Figure 8 are representative raw data obtained with Ch* in PC/ATPase samples for the cholesterol equilibrium binding treatment. Two distinct components are visually detectable in the top three spectra. The broader of these components is attributed to spin-label in contact with the Ca-ATPase surface and the sharper to spin-label in contact only with other lipid molecules. The analysis of the composite line shapes followed the same general strategy used above in analyzing the data obtained with the phospholipid spin-label. The rotationally restricted line shape shown in Figure 9b was first isolated from a composite spectrum. The procedure was to record the spectrum from a sample of relatively low lipid to protein ratio (37 PC's per ATPase; top spectrum of Figure 8) and, using an appropriate bilayer line shape, to remove the more mobile component. The resulting bound reference spectrum shows a remarkably close resemblance to the experimental model system spectrum 9e. For all of the data analysis in this series, the broad component

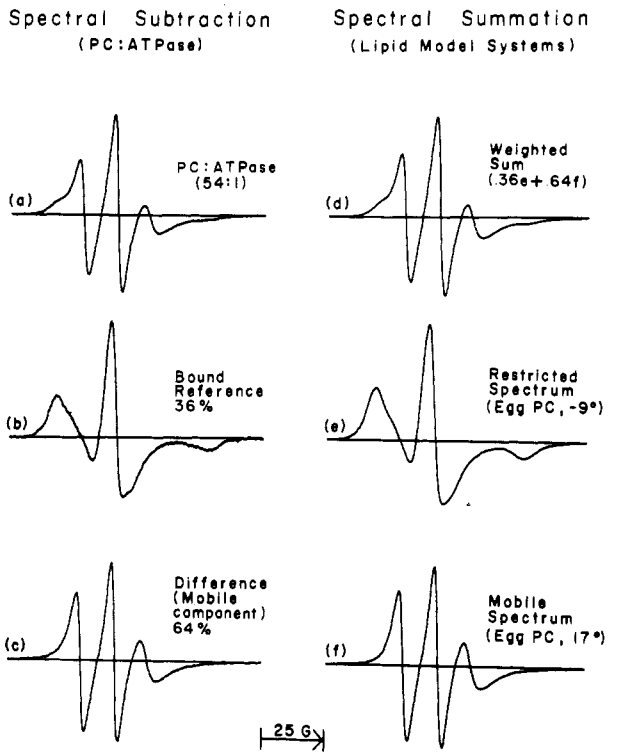

FIGURE 9: Illustration of the Ch* spectral data treatment. The line shapes are very different from those of the PC* data (Figure 4), but the analytic approach is the same. Each experimental spectrum (a) is digitized, and the bound reference spectrum (b) is subtracted, yielding the bilayer difference spectrum (c). The percentage contributions of the integrated intensities of components b and c (in this case 36% and 64%, respectively) are then used to calculate y in the equilibrium binding plots. As in Figure 5 the right column of spectra are matching line shapes from the lipid model systems, where spectrum d is the weighted sum of spectra e and f (Ch* in egg PC at −9 and 17 °C, respectively).

9b was used for the subtractions. The bilayer end points were judged by comparison of the difference spectra with model system line shapes. An example is shown in the bottom two spectra of Figure 9, where the difference spectrum (left) can be compared with the model system reference (right). Figure 9 also illustrates the analysis of a sample containing 54 PC's per ATPase. Appropriate normalization gives the quantitative contribution of each component. The right column of Figure 9 demonstrates that the fractional contribution of each component obtained by subtraction (left column) can be used for summing the model system spectra (9e and 9f) to give a composite spectrum (9d), which is essentially identical with the original experimental spectrum from the PC–ATPase reconstitution (9a).

The results of the spectral subtractions just outlined indicated that a smaller fraction of the cholesterol spin-label than of the PC* spin-label was associated with the Ca-ATPase in PC–ATPase recombinants of a given lipid/protein ratio. For example, the subtraction illustrated on the left side of Figure 9 indicates that 36% of the cholesterol spin-label is associated with the Ca-ATPase in a recombinant with 54 PC's per ATPase. In another recombinant of the same lipid/protein ratio, 46% of the PC* spin-label is in contact with the Ca-ATPase surface (see Figure 6a–c). The results of the quantitative data for Ch* are presented in Figure 10. Because of the point scatter N is not precisely defined but is consistent with the value of ~22, obtained from the PC* data. The average binding constant is less than that of the reference phospholipid, PC, with the solid line corresponding to $K_{av} = 0.65$. For comparison $K_{av} = 0$ (total exclusion of Ch* from the protein

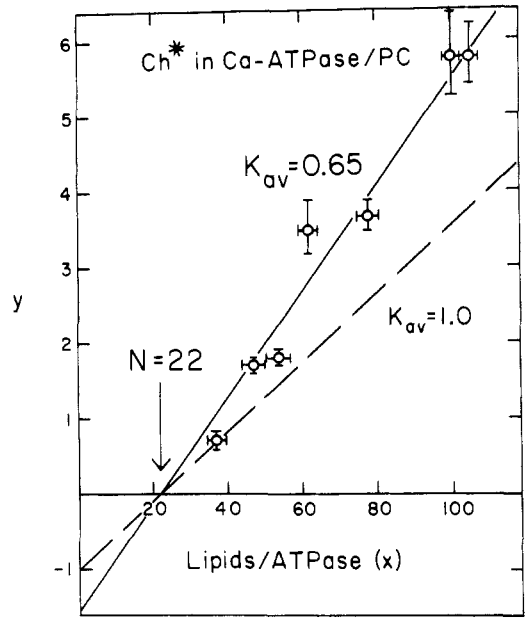

FIGURE 10: Equilibrium binding curve for the cholesterol spin-label Ch* in egg PC/ATPase samples derived from the ESR spectral analysis (y, the free to bound ratio) and compositional data (x, the molar ratio of egg PC/ATPase). The solid line fitting the experimental data corresponds to $N = 22$, and $K_{av} \sim 0.65$. The dashed line is for $N = 22$ and $K_{av} = 1.0$, corresponding to the case of nonspecific binding or solvation (as for PC* in the PC background of Figure 7).

surface) would be a vertical line, passing through $N = 22$. The dashed line shows $K_{av} = 1.0$ (equal competition).

The spin-labeled cholesterol closely resembles the structure of native cholesterol. Nevertheless, it is desirable to examine cholesterol–phospholipid competition using unlabeled cholesterol. For this purpose, lipid/ATPase recombinants were prepared which contained PC* in a background of egg PC containing unlabeled cholesterol. This experimental design, while straightforward in principle, creates complications in the quantitative spectral analysis due to difficulties in generating model line shapes needed to fine tune the subtraction end points. Also, a rigorous quantitative analysis based on an equilibrium binding treatment requires that the activity coefficients of all lipid species be constant over the full range of compositions studied, which is unlikely to be the case when substantial amounts of cholesterol are incorporated into the phospholipid bilayer. Nevertheless, meaningful qualitative trends can be detected. The results of four experiments are given in Table I. The observed percentages of phospholipid spin-label in contact with the protein (column 3) are less than the values calculated by assuming no cholesterol displacement of phospholipid (column 4), indicating that cholesterol is not excluded from the lipid–protein interface. The observed values are, however, consistently larger than those calculated for equal competition at the lipid–protein interface (column 5). The fact that the observed values are intermediate between these two limiting cases is consistent with the equilibrium binding data from Ch* where $0 < K_{av} < 1$ (see Figure 10).

Table I: Competition of Unlabeled Cholesterol with PC* in Reconstituted Ca-ATPase

molar composition		percentage of PC* bound		
			predicted	
PC/ATPase	cholesterol/ATPase	observed[a]	cholesterol[b] excluded	cholesterol[c] equivalent to PC
41	29	43	54	31
54	32	36	41	26
55	31	35	40	26
67	24	28	33	24

[a] PC*/ATPase molar ratio of 0.4 and spectra recorded at 25 °C. Estimated error is ±2 in the subtraction end points. [b] Calculated by dividing the number of sites (22) by column 1 (assumes $K_{Ch} = 0$). [c] Calculated by dividing 22 by the sum of columns 1 and 2 (assumes $K_{Ch} = 1$).

Discussion

Reconstitution. The two-stage reconstitution procedure devised for these experiments accomplished the two main goals of manipulating the lipid to protein ratio (x) of the final sample in a predictable manner and maintaining a constant ratio of the water-insoluble lipid spin-label to the protein (x^*). In the first stage of the reconstitution, the Ca-ATPase of native sarcoplasmic reticulum was purified, and its associated lipids were exchanged for phosphatidylcholine by using cholate (Warren et al., 1974a,b). This procedure avoids delipidation of the protein, minimizing the possibility of irreversible protein–protein aggregation. In the second stage, defined quantities of lipid and lipid spin-label were introduced with octyl glucoside, and complete removal of detergent was accomplished by subsequent dilution and gel filtration. In our hands, this two-step procedure gives reproducible vesicular samples. These samples retained enzymatic activity, were essentially homogeneous in protein and in lipid composition, and gave relatively predictable lipid/protein molar ratios.

Number of Lipid Contact Sites Determined by the Equilibrium Binding Treatment. The quantitative spectral subtractions for PC* in Ca-ATPase/PC recombinants when analyzed according to the equilibrium binding treatment of Brotherus et al. (1981) yield a plot with x intercept of $N = 22 \pm 2$ mol of PC per M_r 115000 protein (see Figure 7), where N is the number of lipid binding (contact) sites on the hydrophobic surface of this transmembranous protein. This analysis assumes that this number is independent of the lipid/protein ratio, an assumption supported by the linearity of the experimental binding plot. To minimize irreversible protein aggregation during the reconstitution, our procedure was designed to ensure that the protein was at no point stripped of phospholipid. Reversible protein–protein contacts could, of course, be formed at high protein concentration in the membrane. However, at the lipid/protein ratios used in this study, any such protein–protein interactions do not appear to influence the extent of lipid association with the protein. Deliberate glutaraldehyde cross-linking of the ATPase in the native membrane has no effect on the amount of lipid contacting the protein surface, judging from the absence of ESR spectral line-shape changes (Thomas et al., 1982). Using the same protocol, we have reproduced these results for both native and reconstituted membranes. If protein–protein contacts occur at high protein concentrations, these appear to involve the extramembranous hydrophilic portions of the Ca-ATPase and not the membrane-penetrating portions of the molecule that interact with the lipid chains.

If the protein forms a functional oligomer, part of the surface of each monomeric unit would be involved in protein–protein contact, so that N is the average number of sites per monomer exposed to the bilayer, rather than a measure of the total surface of the calcium pump. The experimental value of $N \sim 22$ for both the reconstituted samples and the native membrane reported here is consistent with earlier data based on successive lipid depletion of the SR membrane (Nakamura & Ohnishi, 1975; Jost & Griffith, 1978a; Thomas et al., 1982) and within the wide range estimated in two samples by McIntyre et al. (1982). It has been reported that

full Ca-ATPase activity is dependent on the presence of ≳30 phospholipids per ATPase (Warren et al., 1974a,b; Hesketh et al., 1976). This represents fairly good agreement between the spectroscopic and enzymatic results, indicating that the same lipid population is involved and that these lipids in contact with the protein are essential for activity.

Competition between Cholesterol and Phosphatidylcholine. While estimates of the number of lipids in contact with the Ca-ATPase provide a useful contribution to the understanding of the structure and disposition of the protein in the membrane, it is of greater interest to determine to what extent a protein can discriminate between lipids of very different structures. Our analysis of the PC* interactions indicates that the spin-labeled PC* and egg PC interact equally well with the ATPase ($K_{av} = 1$), i.e., that the presence of the nitroxide moiety in PC* does not affect its equilibrium association with the protein. This result agrees with the report of Feigenson and co-workers (Caffrey & Feigenson, 1981; London & Feigenson, 1981), who examined the paramagnetic quenching of Ca-ATPase tryptophan fluorescence by an excess of spin-labeled PC in competition with a large number of non-spin-labeled phosphatidylcholines that varied in acyl chain structure. These authors concluded that phospholipid species of very different acyl chain compositions all interact equally well with Ca-ATPase, so long as the lipids are in the liquid-crystalline state [see Griffith et al. (1982b)]. This conclusion is in agreement with results obtained in other reconstituted systems that have been examined at temperatures above the T_c of the lipids (Griffith & Jost, 1979; Knowles et al., 1979; Cable & Powell, 1980; Brotherus et al., 1981).

While the Ca-ATPase appears to show no specificity for different phospholipid head-group species [East & Lee, 1982; for review, see Roelofsen (1981)], the interaction of cholesterol with the protein can, in principle, be quite different from that of phospholipid. Warren et al. (1975) have in fact concluded from enzymatic activity measurements that, in the presence of sufficient phospholipid to surround the protein, cholesterol is essentially excluded from the protein surface. To examine cholesterol–ATPase interactions in the presence of phosphatidylcholine, we have used two different experimental designs. The first design examined the interaction of a spin-labeled cholesterol (Ch*) with the Ca-ATPase reconstituted with phosphatidylcholine. On the basis of our equilibrium binding results (see Figure 10) cholesterol does, in fact, contact the protein, but with a somewhat lower probability than phosphatidylcholine ($K_{av} < 1$). The experimental value of a relative binding affinity of 0.6–0.7 is consistent with either (1) the exclusion of cholesterol from about one-third of the available contact sites or (2) a lowered probability of cholesterol replacing phospholipid at each site. Both models would predict a linear plot of y vs. x and an extrapolated x intercept of N (Brotherus et al., 1981; Griffith et al., 1982a), as observed in Figure 10. The actual case probably lies between these two extremes, with appreciable heterogeneity in the extent of the discrimination between cholesterol and PC at different contact sites on the lipid-associating surface of the protein.

The essential observation is that there is a lower probability of finding cholesterol at the lipid–protein interface than phospholipid. We can only speculate as to why this is the case. In principle, there are three theoretical possibilities: first, that steric factors make the direct contact of cholesterol with the protein less favorable; second, that there would be a net attraction between phosphatidylcholine and protein relative to cholesterol; third, that there is a weak preferential association of cholesterol and phospholipid that would tend to result in surrounding each cholesterol with phospholipid in the bilayer. The first possibility seems most likely. We note that the experimental value of the relative binding constant ($K_{av} \simeq 0.65$) was determined at very low concentrations of the cholesterol label with no added cholesterol, so that any effects due to high cholesterol concentrations are not a factor.

The structure of the spin-labeled cholesterol used in this study preserves the stereochemistry of the steroid nucleus, the important 3β-hydroxy group, and the hydrocarbon side chain characteristic of cholesterol. The nitroxide group is literally built into the hydrophobic end of the steroid nucleus, minimizing the structural differences with authentic cholesterol. This spin-labeled cholesterol can also substitute for cholesterol in several enzymatic reactions (Keana et al., 1981). Only if the Ca-ATPase could be reconstituted in bilayers of pure cholesterol, which is not physically possible, could the equivalence of spin-labeled and unlabeled cholesterol in cholesterol–protein interactions be tested in the fashion used above for the equivalence of PC* and PC. Therefore, a second experimental design was used to cross-check the association of cholesterol with the protein. This was done by measuring the displacement of PC* from the Ca-ATPase surface by unlabeled cholesterol added to PC–ATPase recombinants. Experimentally, this was accomplished by comparing the amount of protein-associated PC* in a PC–cholesterol–ATPase recombinant with the extent of cholesterol–protein association predicted for both the case of complete exclusion of cholesterol from contact with the protein surface and the case where cholesterol and phosphatidylcholine have equal probabilities of contacting the protein. Our experimental results (Table I) indicate qualitatively that unlabeled cholesterol can displace PC* from the Ca-ATPase surface but not as efficiently as PC. This conclusion is in agreement with the more quantitative results obtained with the cholesterol spin-label discussed here. Both experimental approaches to the question of cholesterol–ATPase interactions indicate that such interactions do occur, even in the presence of PC in excess of the amount required to cover the hydrophobic surface of the enzyme. However, cholesterol clearly interacts somewhat more weakly with Ca-ATPase than does PC.

Our data are not inconsistent with the actual data obtained by Warren et al. (1975), who used different techniques and a very different experimental design. Our results are in limited agreement with the conclusions of Warren et al. (1975), in that we find a somewhat diminished tendency for cholesterol to associate with the protein in the presence of excess phospholipid. But, unlike these authors' conclusions, we do not find evidence for complete exclusion of cholesterol from the hydrophobic surface of the Ca-ATPase, and our data support the conclusion that there is exchange between phospholipid and cholesterol at the lipid–protein interface even at high lipid/protein ratios. Warren et al. (1975) interpreted their data, obtained at very low lipid/protein ratios, as direct inhibition of ATPase activity by cholesterol due to cholesterol occupancy of lipid contact sites on the protein surface. They reasoned that the restoration of full activity by added phospholipid was due to exclusion of cholesterol from contact with the protein, so that cholesterol was no longer inhibitory. An alternate interpretation for their data could be that there was indirect inhibition because cholesterol does not form a hydrophobic milieu of sufficient plasticity to support Ca-ATPase activity until a certain minimum amount of phospholipid is also present. It has in fact been shown that a greatly diminished fluidity in the membrane hydrophobic interior, e.g., in gel phase lipids or at low lipid–protein ratios, leads to major

reductions in ATPase activity (Moore et al., 1978).

Our data, in combination with some of the earlier published data from several laboratories, form a consistent picture of lipid–protein interactions involving the Ca-ATPase both in reconstituted systems and in the native sarcoplasmic reticulum. The lipids in these membranes are in dynamic equilibrium. There is lateral diffusion of the lipids in the plane of the bilayer, and lipid is exchanging between the protein boundary and the bilayer. The influence of the protein on phospholipid chain dynamics is very pronounced when the lipid directly contacts the protein surface, with subtler influences propagated further out into the bilayer. The lipid in contact with protein is motionally restricted. The motionally restricted component for the PC* spin-label in this system exhibits slightly more motion, reflected both in the line shape and in a smaller splitting (~57.5 G), than has been previously reported for the same label in contact with Na,K-ATPase from electric eel [~61 G (Brotherus et al., 1980)] and cytochrome oxidase [~63 G (P. C. Jost, unpublished data)]. These measured splittings are much less than the rigid-glass limit of 69.2 G (measured for 14-proxylstearic acid bound to cytochrome oxidase at 77 K), indicating that PC* in contact with sarcoplasmic reticulum Ca-ATPase is not rigidly immobilized but exhibits some motion on the ESR time scale. The spectral line shape observed for the ATPase-associated component of the cholesterol spin-label is characteristic of strongly hindered rotation about the long molecular axis but again does not indicate on the ESR time scale a total immobilization of this label when in contact with the protein.

In summary, the transmembranous Ca-ATPase in egg PC bilayers and in the native sarcoplasmic reticulum membrane has ~22 lipid contact sites available per monomeric unit. Cholesterol is not excluded from contact with the hydrophobic protein surface, but the probability of interaction is somewhat lower than for phosphatidylcholine. One plausible basis for this difference in lipid–protein interactions is that the rigid steroid structure of cholesterol cannot conform as well to the irregular surface of the protein as can the flexible phospholipid side chains.

Acknowledgments

We thank Dr. Giuseppe Inesi (University of Maryland School of Medicine) for useful discussions on preparation of the sarcoplasmic reticulum from rabbit muscle.

Registry No. I, 78709-94-1; II, 78228-58-7; III, 57-88-5; ATPase, 9000-83-3.

References

Banerjee, R., Epstein, M., Kandrach, M., Zimniak, P., & Racker, E. (1979) *Membr. Biochem. 2*, 283–296.

Bangham, A. D., Hill, M. W., & Miller, N. G. A. (1974) in *Methods of Membrane Biology* (Korn, E. D., Ed.) pp 1–68, Plenum Press, New York.

Bennett, J. P., Smith, G. A., Houslay, M. D., Hesketh, T. R., Metcalfe, J. C., & Warren, G. B. (1978) *Biochim. Biophys. Acta 513*, 310–320.

Bligh, E. G., & Dyer, W. J. (1959) *Can. J. Biochem. Physiol. 37*, 911–917.

Brotherus, J. R., Jost, P. C., Griffith, O. H., & Hokin, L. E. (1979) *Biochemistry 18*, 5043–5050.

Brotherus, J. R., Jost P. C., Griffith, O. H., Keana, J. F. W., & Hokin, L. E. (1980) *Proc. Natl. Acad. Sci. U.S.A. 77*, 272–276.

Brotherus, J. R., Griffith, O. H., Brotherus, M. O., Jost, P. C., Silvius, J. R., & Hokin, L. E. (1981) *Biochemistry 20*, 5261–5267.

Cable, M. B., & Powell, G. L. (1980) *Biochemistry 19*, 5679–5686.

Caffrey, M., & Feigenson, G. W. (1981) *Biochemistry 20*, 1949–1961.

Champeil, P., Buscheln, S., & Guillain, F. (1981) *Biochemistry 20*, 1520–1524.

Davis, P. J., Coolbear, K. P., & Keough, K. M. W. (1980) *Can. J. Biochem. 58*, 851–858.

Dean, W., & Tanford, C. (1977) *J. Biol. Chem. 253*, 3551–3553.

Deese, A. J., Dratz, E. A., Hymel, L., & Fleischer, S. F. (1982) *Biophys. J. 37*, 207–216.

East, J. M., & Lee, A. G. (1982) *Biochemistry 21*, 4144–4151.

Eletr, S., & Inesi, G. (1972) *Biochim. Biophys. Acta 282*, 174–179.

Gomez-Fernandez, J. C., Goñi, F. M., Bach, D., Restall, C. J., & Chapman, D. (1980) *Biochim. Biophys. Acta 598*, 502–516.

Griffith, O. H., & Jost, P. C. (1979) in *Cytochrome Oxidase* (King, T. E., Chance, B., Okunuki, K., & Orii, Y., Eds.) pp 207–217, Elsevier/North-Holland Biomedical Press, Amsterdam.

Griffith, O. H., Brotherus, J. R., & Jost, P. C. (1982a) in *Lipid-Protein Interactions* (Jost, P. C., & Griffith, O. H., Eds.) pp 225–237, Wiley-Interscience, New York.

Griffith, O. H., Baumeister, J. C., & Jost, P. C. (1982b) *Biophys. J. 37*, 152–154.

Hardwick, P. M. D., & Green, N. M. (1974) *Eur. J. Biochem. 42*, 183–193.

Hesketh, T. R., Smith, G. A., Houslay, M. D., McGill, K. A., Birdsall, N. J. M., Metcalfe, J. C., & Warren, G. B. (1976) *Biochemistry 15*, 4145–4151.

Jost, P. C., & Griffith, O. H. (1978a) in *Biomolecular Structure and Function* (Agris, P. F., Ed.) pp 25–54, Academic Press, New York.

Jost, P. C., & Griffith, O. H. (1978b) *Methods Enzymol. 49*, 369–418.

Keana, J. F. W. (1979) in *Spin Labeling: Theory and Applications* (Berliner, L. J., Ed.) pp 115–172, Academic Press, New York.

Keana, J. F. W., Tamura, T., McMillen, D. A., & Jost, P. C. (1981) *J. Am. Chem. Soc. 103*, 4904–4912.

Keana, J. F. W., Boyd, S. A., McMillen, D. A., Bernard, E. M., & Jost, P. C. (1982) *Chem. Phys. Lipids 31*, 339–349.

Knowles, P. F., Watts, A., & Marsh, D. (1979) *Biochemistry 18*, 4480–4487.

Knowles, P. F., Watts, A., & Marsh, D. (1981) *Biochemistry 20*, 5888–5894.

Laemmli, U. K. (1970) *Nature (London) 227*, 680–689.

London, E., & Feigenson, G. W. (1981) *Biochemistry 20*, 1939–1948.

Lowry, D. H., Rosebrough, N. J., Farr, A. L., & Randall, R. J. (1951) *J. Biol. Chem. 193*, 265–275.

Lowry, R. J., & Tinsley, I. J. (1974) *Lipids 9*, 491–492.

MacLennan, D. H. (1974) *Methods Enzymol. 32*, 291–302.

Marai, L., & Kuksis, A. (1973) *Can J. Biochem. 51*, 1248–1261.

Marsh, D., & Watts, A. (1982) in *Lipid-Protein Interactions* (Jost, P. C., & Griffith, O. H., Eds.) pp 53–126, Wiley-Interscience, New York.

Marsh, D., Watts, A., Maschke, W., & Knowles, P. F. (1978) *Biochem. Biophys. Res. Commun. 81*, 397–402.

McIntyre, O., Samson, P., Brenner, S. C., Dalton, L., Dalton, L., & Fleischer, S. (1982) *Biophys. J. 37*, 53–56.

McLaughlin, A. C., Herbette, L., Blasie, J. K., Wang, C. T., Hymel, L., & Fleischer, S. (1981) *Biochim. Biophys. Acta 643*, 1–16.
Meissner, G. (1974) *Methods Enzymol. 31*, 238–246.
Mimms, L. T., Zampighi, G., Nozaki, Y., Tanford, C., & Reynolds, J. A. (1981) *Biochemistry 20*, 833–840.
Moore, B. M., Lentz, B. R., & Meissner, G. (1978) *Biochemistry 17*, 5248–5255.
Nakamura, M., & Ohnishi, S.-I. (1975) *J. Biochem. (Tokyo) 78*, 1039–1045.
Parsons, J. G., & Patton, S. (1967) *J. Lipid Res. 8*, 696.
Rice, D. M., Meadows, M. D., Scheinman, A. O., Goñi, F. M., Gomez-Fernandez, J. C., Moscarello, M. A., Chapman, D., & Oldfield, E. (1979) *Biochemistry 18*, 5893–5903.
Roelofsen, B. (1981) *Life Sci. 29*, 2235–2247.
Roman, R., & Keana, J. F. W. (1978) *Membr. Biochem. 1*, 323–327.
Sanslone, W. R., Bertrand, H. A., Yu, S. P., & Masero, E. J. (1972) *J. Cell. Physiol. 79*, 97–102.
Seelig, J., Tamm, L., Hymel, L., & Fleischer, S. (1981) *Biochemistry 20*, 3922–3932.
Singelton, W. S., Gray, M. S., Brown, M. L., & White, J. L. (1965) *J. Am. Oil Chem. Soc. 42*, 53–56.
Stoffel, W., Zierenberg, O., & Scheefers, M. (1977) *Hoppe-Seyler's Z. Physiol. Chem. 358*, 865–882.
Thomas, D. D., Bigelow, D. J., Squier, T. C., & Hidalgo, C. (1982) *Biophys. J. 37*, 217–225.
Van, S. P., Birrell, G. B., & Griffith, O. H. (1974) *J. Magn. Reson. 15*, 444–459.
Wang, C.-T., Saito, A., & Fleischer, S. (1979) *J. Biol. Chem. 254*, 9209–9219.
Warren, G. B., Toon, P. A., Birdsall, N. H. M., Lee, A. G., & Metcalfe, J. C. (1974a) *Biochemistry 13*, 5501–5507.
Warren, G. B., Toon, P. A., Birdsall, N. J. M., Lee, A. G., & Metcalfe, J. C. (1974b) *Proc. Natl. Acad. Sci. U.S.A. 71*, 622–626.
Warren, G. B., Houslay, M. D., Metcalfe, J. C., & Birdsall, N. J. M. (1975) *Nature (London) 255*, 684–687.

In Vitro Exchange of Nucleosomal Histones H2a and H2b†

Larry Louters and Roger Chalkley*

ABSTRACT: We have asked whether exogenous, radiolabeled histones can exchange with nucleosomal histones in an in vitro system. Using two different electrophoretic techniques, we were able to separate the histones contained in nucleosomes from those histones which were simply bound to the surface of the chromatin. Fluorography was used to determine which of the exogenous histones exchange with the nucleosomal histones. We observed substantial exchange of histones H1, H2a, and H2b when the chromatin and exogenous histones were incubated under approximately physiological conditions. We have also observed a small amount of exchange of H2a and H2b, as well as a substantial exchange of H1, from one chromatin fragment to another. Other conditions affecting the exchange of histones H2a and H2b are also reported.

The nucleosome is a fundamental unit of chromatin structure. Initially, the nucleosome was viewed as a largely static structure with histone octamers remaining intact and associated with the same stretch of DNA throughout the lifetime of the cell. However, the need for a measure of plasticity in this structure is likely in view of the nuclear metabolic events which require DNA as a template. One measure of the dynamic nature of the nucleosome structure would be the ability of histones to exchange in and out of the nucleosome. We have investigated this possibility directly.

Three lines of evidence led us to expect that exogenous histones might exchange into nucleosomes. First, it is now clear that there is a measure of continued histone synthesis throughout the cell cycle (Groppi & Coffino, 1980; Shenin & Lewis, 1980; Tarnowka et al., 1978; Waithe et al., 1983; Wu & Bonner, 1981). These histones synthesized in the absence of DNA replication have been shown to be associated with chromatin, which may indicate that they have exchanged with nucleosomal histones (Nadeau et al., 1978; Russev et al., 1980; Russev & Hancock, 1981). Second, newly synthesized histones H1, H2a, and H2b are not deposited specifically on new DNA but are somewhat randomized, leading to the suggestion that these histones can exchange with a histone pool, possibly nucleosomal in origin (Jackson & Chalkley, 1981a,b). Third, it has been clearly demonstrated that histone H1 can exchange in vitro at relatively low ionic strength (Caron & Thomas, 1981).

In this report, we have investigated the possibility of in vitro exchange between exogenous core histones and nucleosomal histones. By two separate methods, one based on isolation of the internal octamer and the other on isolation of nucleosomes, we conclude that core histones H2a and H2b, as well as histone H1, can undergo substantial exchange. In addition to observing the exchange of exogenous histones with nucleosomal histones, we have also observed a very small amount of exchange of histones H2a and H2b, as well as an extensive exchange of H1, from chromatin to chromatin.

Materials and Methods

Generation and Isolation of [^{3}H]Lysine-Labeled Histones. HTC cells were grown for 2–3 generations in Swims S-77 with serum plus 2–3 mCi of [^{3}H]lysine per L. Cells were collected by centrifugation at 400*g* for 5 min and frozen. The cells were washed 4 times in washing buffer [10 mM tris(hydroxymethyl)aminomethane (Tris),[1] pH 7.5, 10 mM $MgCl_2$, 0.25

† From the Department of Biochemistry, College of Medicine, University of Iowa, Iowa City, Iowa 52242. *Received August 5, 1983.* This work was supported by grants from the National Institutes of Health to R.C. (Grant GM 28817) and to the Diabetes and Endocrinology Research Center (Grant AM 25295). L.L. was supported by NIH Training Grant GM 07045-05.

0006-2960/84/0423-0547$01.50/0